Int J Heat Mass Transfer Vol 20, pp. 171–173. Pergamon Press 1977. Printed in Great Britain

SHORTER COMMUNICATIONS

HEAT TRANSFER TO PULSATILE FLOW IN A POROUS CHANNEL

G. RADHAKRISHNAMACHARYA and M. K. MAITI
Department of Mathematics, Indian Institute of Technology, Kharagpur, India

(*Received* 28 *October* 1975 *and in revised form* 14 *April* 1976)

NOMENCLATURE

A, constant defined in (1);
ε, suitably chosen positive quantity;
p, pressure;
ρ, density;
ω, frequency;
t, time;
x, y, Cartesian coordinates;
μ, coefficient of viscosity;
ν, kinematic coefficient of viscosity;
u, velocity component in the x-direction;
v, injection velocity;
T, temperature of the fluid;
T_0, T_1, constant temperatures of the walls;
h, distance between the walls;
c, specific heat;
g, acceleration due to gravity;
k, thermal conductivity;
u_0, u_1, non-dimensional velocity components given by (7a) and (7b);
R, vh/ν, cross flow Reynolds number;
M, $h(\omega/\nu)^{1/2}$, frequency parameter;
η, y/h, dimensionless distance;
θ, $\dfrac{T-T_0}{T_1-T_0}$, dimensionless temperature;
$\theta_0(\eta)$, non-dimensional steady temperature;
$F(\eta), G(\eta)$, non-dimensional functions defined in (12) and (13);
Pr, $\mu gc/k$, Prandtl number;
Ec, $(Ah^2/\nu)^2/gc(T_1-T_0)$, Eckert number;
Q_0, heat transfer at the injection wall;
Q_1, heat transfer at the suction wall;
$|D_0|, |D_1|$, amplitudes of rate of heat transfer at the injection and suction walls;
α_0, α_1, phases of rate of heat transfer at the injection and suction walls.

1. INTRODUCTION

THE PROBLEMS of fluid flow in a porous pipe and channel have been studied in recent past by many workers [1–5] with a view to understanding some practical phenomena like transpiration cooling and gaseous diffusion. Particularly the pulsatile flow in a porous channel is important in the dialysis of blood in artificial kidneys [7]. The present paper considers the heat transfer to the pulsatile flow in a porous channel, treating blood as a Newtonian viscous fluid [8].

2. MATHEMATICAL ANALYSIS

Consider the pulsatile flow of fluid between two infinitely long parallel and porous plates, distant h apart, which is driven by the unsteady pressure gradient

$$-\frac{1}{\rho}\frac{\partial p}{\partial x} = A\{1+\varepsilon\exp(i\omega t)\}, \tag{1}$$

where A is a known constant, ε is a suitably chosen positive quantity and ω is the frequency. Let the x-axis be along one plate and the y-axis normal to it. The plates $y = 0$ and $y = h$ are maintained at uniform temperatures T_0 and T_1 respectively. On one plate some fluid is injected with a velocity v and removed at the opposite plate at the same rate. So, with the help of the continuity equation, the momentum equation and the energy equation reduce to

$$\frac{\partial u}{\partial t}+v\frac{\partial u}{\partial y} = -\frac{1}{\rho}\frac{\partial p}{\partial x}+\nu\frac{\partial^2 u}{\partial y^2}, \tag{2}$$

$$0 = -\frac{1}{\rho}\frac{\partial p}{\partial y}, \tag{3}$$

$$\rho gc\left[\frac{\partial T}{\partial t}+v\frac{\partial T}{\partial y}\right] = k\frac{\partial^2 T}{\partial y^2}+\mu\left(\frac{\partial u}{\partial y}\right)^2, \tag{4}$$

where all the variables have their usual meaning. The boundary conditions are

$$\left.\begin{array}{l} u = 0,\ T = T_0 \quad \text{at} \quad y = 0 \\ u = 0,\ T = T_1 \quad \text{at} \quad y = h. \end{array}\right\} \tag{5}$$

The solution of (2) is in the form;

$$u = \frac{Ah^2}{\nu}[u_0+\varepsilon u_1\exp(i\omega t)]. \tag{6}$$

where u_0 and u_1 are already given by Berman [5] and Wang [6] respectively as

$$u_0 = \frac{1}{R}\left[\frac{\exp(R\eta)-1}{\exp(R)-1}-\eta\right], \tag{7a}$$

$$u_1 = \frac{i}{M^2} \times\left[1+\frac{\{1-\exp(m_2)\}\exp(m_1\eta)-\{1-\exp(m_1)\}\exp(m_2\eta)}{\exp(m_2)-\exp(m_1)}\right], \tag{7b}$$

where $m_{1,2} = \frac{1}{2}[R\pm(R^2+4iM^2)^{1/2}] = A_{1,2}\pm iB_1$, $\eta = y/h$, $R(=vh/\nu)$ is the cross flow Reynolds number and M is a new non-dimensional parameter $h(\omega/\nu)^{1/2}$ characterising the frequency. Introducing the non-dimensional temperature

$$\theta = \frac{T-T_0}{T_1-T_0},$$

equations (4) and (5) become

$$\rho gc\left[\frac{\partial\theta}{\partial t}+\frac{v}{h}\frac{\partial\theta}{\partial\eta}\right] = \frac{k}{h^2}\frac{\partial^2\theta}{\partial\eta^2}+\frac{\mu}{h^2(T_1-T_0)}\left(\frac{\partial u}{\partial\eta}\right)^2, \tag{8}$$

$$\left.\begin{array}{l} \theta = 0 \quad \text{at} \quad \eta = 0, \\ \theta = 1 \quad \text{at} \quad \eta = 1. \end{array}\right\} \tag{9}$$

In view of (6), the temperature θ can be assumed to have the form

$$\theta(\eta, t) = \theta_0(\eta)+\varepsilon F(\eta)\exp(i\omega t)+\varepsilon^2 G(\eta)\exp(2i\omega t). \tag{10}$$

On substituting (10) and (6) in (8), equating harmonic terms, retaining coefficients of ε^2, and solving the corresponding differential equations with the help of (7), we get

$$\theta_0(\eta) = C_1 + C_2\exp(PrR\eta) - \frac{PrEc}{R^2}\left[\frac{\exp(2R\eta)}{2(2-Pr)\{\exp(R)-1\}^2} - \frac{\eta}{PrR} - \frac{2\exp(R\eta)}{R(1-Pr)\{\exp(R)-1\}} + \frac{\varepsilon^2}{2}\left\{\frac{L_1\exp(2A_1\eta)}{4A_1^2-2A_1PrR} + \frac{L_2\exp(2A_2\eta)}{4A_2^2-2A_2PrR} + \frac{\exp[(A_1+A_2)\eta]}{4B_1^2S_1^2+S_2^2}\left[(2L_3B_1S_1+L_4S_2)\sin 2B_1\eta + (L_3S_2-2L_4B_1S_1)\cos 2B_1\eta\right]\right\}\right], \quad (11)$$

$$F(\eta) = C_3\exp(\lambda_1\eta) + C_4\exp(\lambda_2\eta) + \frac{2iPrEc}{(1-Pr)RM^2\{\exp(m_2)-\exp(m_1)\}} \times \left[\frac{\{1-\exp(m_2)\}\exp(m_1\eta)}{m_1} - \frac{\{1-\exp(m_1)\}\exp(m_2\eta)}{m_2} - \frac{R(1-Pr)\exp(R\eta)}{\exp(R)-1}\{n_1\exp(m_1\eta) - n_2\exp(m_2\eta)\}\right], \quad (12)$$

$$G(\eta) = C_5\exp(\lambda_3\eta) + C_6\exp(\lambda_4\eta) + \frac{PrEc}{4M^4(2-Pr)\{\exp(m_2)-\exp(m_1)\}^2} \times [\{1-\exp(m_2)\}^2\exp(2m_1\eta) + \{1-\exp(m_1)\}^2\exp(2m_2\eta) - 2(2-Pr)n_3\exp(R\eta)], \quad (13)$$

where

$$L_{1,2} = (A_{1,2}^2 + B_1)\{1+\exp(2A_{2,1}) - 2\exp(A_{2,1})\cos B_1\}/NM^2,$$

$$L_{3,4} = 2\{-(A_1B_1 + A_2B_1)M_{2,1} \pm (A_1A_2 - B_1^2)M_{1,2}\}/NM^2,$$

$$M_{1,2} = 1,0 \mp \{\exp(A_1)+\exp(A_2)\}\cos B_1, \sin B_1 \pm \{\exp(A_1+A_2)\}\cos 2B_1, \sin 2B_1,$$

$$S_1 = 2A_1 + 2A_2 - PrR,$$

$$S_2 = \{(A_1+A_2)(A_1+A_2-PrR) - 4B_1^2\}^2,$$

$$N = \exp(2A_1) + \exp(2A_2) - 2\exp(A_1+A_2)\cos 2B_1,$$

$$n_{1,2} = \frac{m_{1,2}\{1-\exp(m_{2,1})\}}{(1-Pr)(R+m_{1,2})^2 + 2PrRm_{1,2}},$$

$$n_3 = \frac{2m_1m_2\{1-\exp(m_1)\}\{1-\exp(m_2)\}}{(1-Pr)R^2 + 2Prm_1m_2},$$

$$\lambda_{1,2} = \tfrac{1}{2}[PrR \pm (Pr^2R^2 + 4iPrM^2)^{1/2}], \quad (14)$$

$$\lambda_{3,4} = \tfrac{1}{2}[PrR \pm (Pr^2R^2 + 8iPrM^2)^{1/2}],$$

$$Pr = \mu gc/k, \quad Ec = (Ah^2/\nu)^2/gc(T_1 - T_0).$$

The expressions for the constants of integration C_1, C_2, C_3, C_4, C_5 and C_6 are not given as they are too complicated.

The rate of heat transfer per unit area at the injection wall is given by

$$Q_0 = \frac{-q_0 h}{k(T_1-T_0)} = \left(\frac{\partial\theta}{\partial\eta}\right)_{\eta=0} = \left.\frac{d\theta_0}{d\eta}\right|_{\eta=0} + \varepsilon\exp(i\omega t)\left.\frac{dF}{d\eta}\right|_{\eta=0} + \ldots. \quad (15)$$

Equation (15) can also be written as

$$Q_0 = \left.\frac{d\theta_0}{d\eta}\right|_{\eta=0} + \varepsilon|D_0|\cos(\omega t + \alpha_0) + \ldots, \quad (15a)$$

where $D_0 (= D_{0r} + iD_{0i})$, the coefficient of $\varepsilon\exp(i\omega t)$ in (15), and $\tan\alpha_0 (= D_{0i}/D_{0r})$ are the amplitude and phase of the rate of heat transfer respectively. Similarly the rate of heat transfer at the suction wall is given by

$$Q_1 = -\frac{q_1 h}{k(T_1-T_0)} = \left.\frac{d\theta_0}{d\eta}\right|_{\eta=1} + \varepsilon|D_1|\cos(\omega t + \alpha_1) + \ldots, \quad (16)$$

where

$$D_1 = D_{1r} + iD_{1i} = \left.\frac{dF}{d\eta}\right|_{\eta=1}$$

and $\tan\alpha_1 = D_{1i}/D_{1r}$. The numerical values of $|D_0|$, $|D_1|$, $\tan\alpha_0$ and $\tan\alpha_1$ are entered in Table 2.

3. DISCUSSIONS

The steady temperature profiles are plotted in Fig. 1. The profiles are almost parabolic and there is no change in the character of the profiles as Ec varies. But, as Eckert number Ec increases, the steady temperature increases. The effect of Eckert number Ec on the steady heat-transfer coefficients is shown in Table 1.

Table 1. ($Pr = 3$, $R = 1$, $M = 10$, $\varepsilon = 1$)

	$Ec = 1$	$Ec = 2$	$Ec = 5$
$(\theta_0')_{\eta=0}$	0.233	0.308	0.531
$(\theta_0')_{\eta=1}$	−1.440	−3.199	−8.993

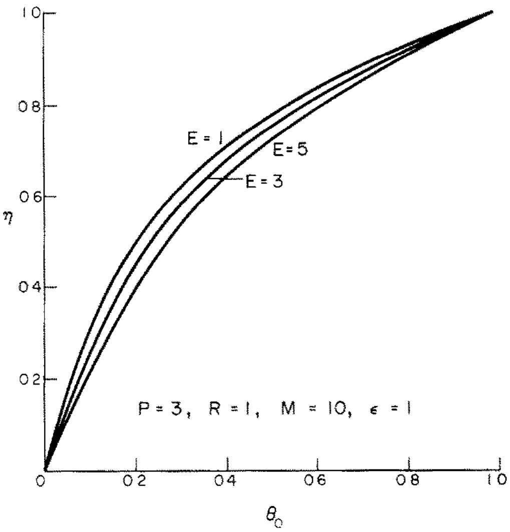

FIG. 1. Steady temperature profiles.

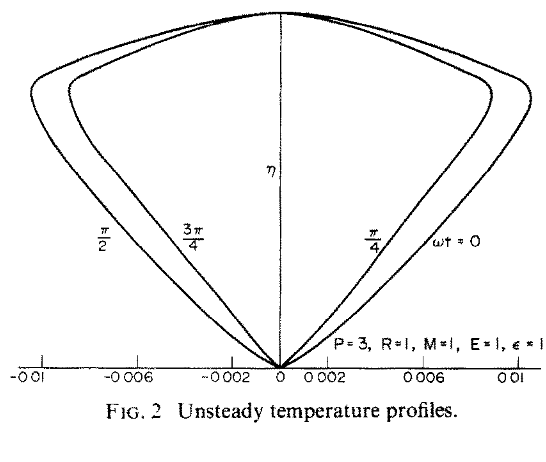

FIG. 2. Unsteady temperature profiles.

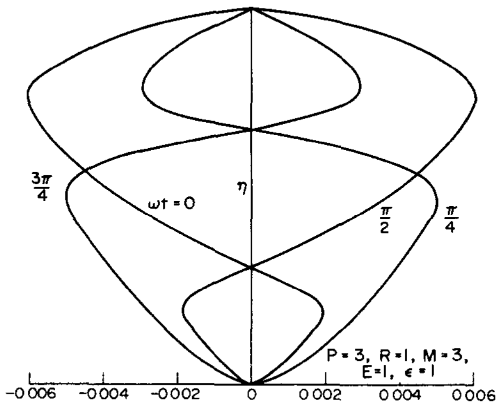

FIG. 3. Unsteady temperature profiles.

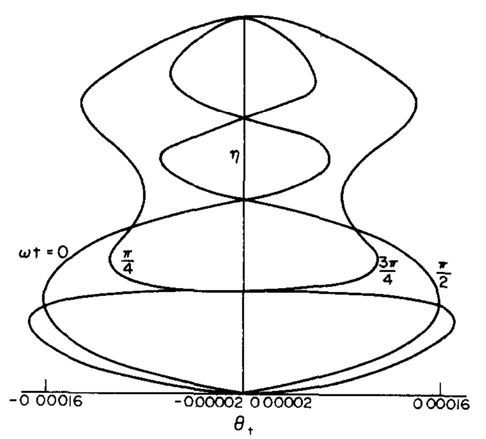

FIG. 4. Unsteady temperature profiles.

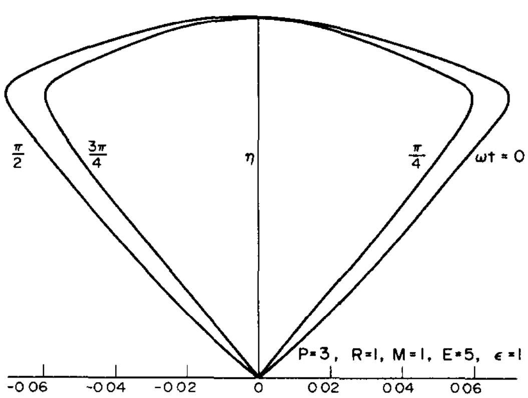

FIG. 5. Unsteady temperature profiles.

We observed that the rate of heat transfer from the injection wall increases with Ec while at the suction wall heat flows from the fluid to the plate even if $T_1 > T_0$.

Fixing Pr and R, the instantaneous temperature profiles are plotted (Figs. 2–5) to observe the effect of changing M (with Ec fixed) and changing Ec (with M fixed). From Figs. 2–4, it can be seen that the temperature decreases as M increases. The temperature profiles are almost parabolic for small values of M, but oscillate more for large values of M and the maximum temperature is shifted to the boundary layers near the walls. The temperature increases rapidly with increase in Ec, which may be due to high viscous dissipation. Part of the temperature profiles are linear and the maximum occurs in the boundary layers near the suction wall (Figs. 2, 5). It can be observed that there is no significant change in the character of the profiles as Ec varies.

The effect of changing M (for fixed Ec) and changing Ec (for fixed M) on the values of the amplitude and phase of the rate of heat transfer is shown in Table 2.

Table 2. ($Pr = 3$, $R = 1$)

		E		
M	1 Values of $\lvert D_0 \rvert$	1 Values of $\lvert D_1 \rvert$	1 Values of $\tan \alpha_0$	1 Values of $\tan \alpha_1$
1	1.1000	2.0140	0.2607	−0.1919
3	0.2476	1.8301	0.1930	1.3740
4	0.0926	0.3027	−0.0560	3.0140
10	0.0070	0.0169	−1.3271	3.6310
		M		
E	1	1	1	1
2	2.1130	4.0925	0.2607	−0.1919
3	3.1730	6.0443	0.2607	−0.1919
4	4.2304	8.0591	0.2663	−0.1952

It may be observed that at the injection wall there is phase lag at higher frequency, but at the suction wall there is a phase lead. It is also to be noted that there is no effect of Ec on the phase at both the walls. We also notice that at the injection wall the amplitude decreases with frequency uniformly for fixed Ec, but at the suction wall it decreases suddenly by 83.6% when M is changed from 3 to 4. For fixed M the amplitude increases uniformly with Ec at both the walls.

Acknowledgements—The authors wish to thank Prof. R. S. Nanda for useful discussion on certain points and to the referees for their valuable comments.

REFERENCES

1. A. S. Berman, Laminar flow in channels with porous walls, *J. Appl. Phys.* **24**, 1232–1235 (1953).
2. J. R. Sellars, Laminar flow in channels with porous walls at high suction Reynolds numbers, *J. Appl. Phys.* **26**, 489–490 (1955).
3. S. W. Yuan, Further investigation in laminar flow in channels with porous walls, *J. Appl. Phys.* **27**, 267–269 (1956).
4. M. Morduchow, On laminar flow through a channel or tube with injection—application of method of averages, *Q. J. Appl. Math.* **14**, 361–368 (1956).
5. A. S. Berman, Laminar flow in an annulus with porous walls, *J. Appl. Phys.* **29**, 71–75 (1958).
6. Y. C. Wang, Pulsatile flow in a porous channel, *J. Appl. Mech.* **38**, 553–555 (1971).
7. W. G. Esmond and H. Clark, Mathematical analysis and mass transfer optimization of a compact, low cost, pumples system for hemodialysis (Dialung), in *Proceedings, Biomedical Fluid Mechanics Symposium.* ASME, New York (1966).
8. J. S. Lee and Y. C. Fung, Flow in locally constricted tubes at low Reynolds numbers, *J. Appl. Mech.* **37**, 9–16 (1970).